Biennial and Lower-Frequency Variability Observed in the Early Summer Climate in the Western North Pacific

TOMOHIKO TOMITA

Department of Environmental Sciences, Kumamoto University, Kumamoto, and Frontier Research Center for Global Change, Japan Agency for Marine-Earth Science and Technology, Yokohama, Japan

TAKAO YOSHIKANE

Frontier Research Center for Global Change, Japan Agency for Marine-Earth Science and Technology, Yokohama, Japan

TETSUZO YASUNARI

Frontier Research Center for Global Change, Japan Agency for Marine-Earth Science and Technology, Yokohama, and Hydrospheric Atmospheric Research Center, Nagoya University, Nagoya, Japan

(Manuscript received 4 April 2003, in final form 16 April 2004)

ABSTRACT

Early summer climate in the western North Pacific is largely represented by the baiu phenomenon. The meridional fluctuations of the baiu front on interannual time scales and the associated large-scale circulations are examined using the empirical orthogonal function (EOF) analysis and composite or correlation analyses based on the EOF time coefficients.

The first EOF mode indicates a 5- or 6-yr low-frequency fluctuation (LF mode) appearing south of 35°N. The development is concurrent with horseshoe sea surface temperature anomalies (SSTAs) in the entire tropical Pacific that are associated with the El Niño–Southern Oscillation (ENSO). SSTAs in the western North Pacific control the anomalous southward expansion of the baiu front through a modification of the convection at around 20°–35°N. The LF mode is negatively correlated with the south-southeast Asian summer monsoon.

The second EOF mode is characterized by a meridional seesawlike fluctuation with a node at around 28°N and a time scale of biennial oscillation (BO mode). The horseshoe SSTAs again control the anomalous meridional circulations, but with a different spatial phase through a convection off the Philippines. The spatial phase difference between the two horseshoe patterns is about 90° in both the zonal and meridional directions. The BO mode is negatively correlated with the tropical western North Pacific monsoon.

SSTAs associated with the BO mode tend to be confined to the tropical western Pacific, while the signals of the LF mode extend rather broadly in the tropical Pacific–Indian Ocean sector, suggesting that the tropical BO is an aborted ENSO in the tropical central–western Pacific. The spatial phase of horseshoe SSTAs adjusts the interannual variability of the meridional fluctuation of the baiu front in the western North Pacific.

1. Introduction

Early summer climate in the western North Pacific is characterized by a locally specified monsoon off the Philippines and by the ''*baiu*'' (in Japanese, ''*mei-yu*'' in Chinese, ''*changma*'' in Korean) phenomenon to the north (Murakami and Matsumoto 1994). Precipitation in the baiu season is, in fact, a prerequisite for summer water resources in East Asia. This work examines the interannual variability of the baiu system in the western North Pacific.

The baiu front, which appears from early June through late July near Japan, climatologically extends along the northwestern periphery of the North Pacific subtropical high (the Pacific high) as part of the Asian summer monsoon (Fig. 1, Murakami and Matsumoto 1994; Wang and LinHo 2002). A large meridional temperature gradient in the midlatitudes, which implies a large baroclinicity and the resultant westerly thermal-wind jet in the upper troposphere, confines the latitudinal location of the baiu front to midlatitudes in the first order. In addition, superimposed variations of the Pacific high and the Okhotsk high to the north modify the characteristics of the baiu front in the western North Pacific (Ninomiya and Mizuno 1987). The development of a large-scale heat low over the Asian continent, which is synchronized with the annual cycle of the sun and seasonally directs moisture from the Tropics to the mid-

Corresponding author address: Dr. Tomohiko Tomita, Department of Environmental Sciences, Faculty of Science, Kumamoto University, Kumamoto 860-8555, Japan.
E-mail: tomita@sci.kumamoto-u.ac.jp

latitudes, is a significant factor in determining the seasonal march of the baiu front (Kawamura and Murakami 1998). Multiscale features in and around the baiu front are well summarized in Ninomiya and Akiyama (1992), and the climatological seasonal march of baiu is comprehensively described by Yoshino (1965, 1966). Large-scale circulations control both spatial and temporal developments of the baiu phenomenon.

The unique nature of the baiu phenomenon, as well as society's deep concern over its impact on water resources, has attracted the attention of a large number of researchers. Weather forecasting, of course, is concerned with baiu precipitation, and the latest regional forecast models provide practical predictions on a synoptic scale. However, general circulation models (GCMs) still fail to simulate a realistic baiu front (Kawatani and Takahashi 2003). To extend the prediction and understand the process of interannual variability, it is necessary to broaden our field of vision to a larger scale and recognize the baiu phenomenon as part of the global climatic system. In particular, it is critical to understand the physical linkage with the main part of the Asian summer monsoon and with the El Niño–Southern Oscillation (ENSO), which is the most outstanding interannual variation in the world.

The baiu activity demonstrates a significant interannual variation, and the baiu rainfall shows a significant correlation with the ENSO cycle that is indicated by the sea surface temperature anomalies (SSTAs) in Niño-3 (4°S–4°N, 150°–90°W; Tanaka 1997). In other words, the baiu precipitation tends to be large in the early summers after the withdrawal of El Niño events, concurrent with an anomalously weak tropical western North Pacific (TWNP) monsoon. Wang et al. (2000) and Wang and Zhang (2002) proposed a physical mechanism whereby the ENSO affects the following summer climate in East Asia through a modification of the TWNP monsoon; in their proposal, they emphasized a specific air–sea interaction with the horseshoe SSTAs extending through the entire tropical Pacific. Diagnosing the output from GCM experiments, Lau and Nath (2000) suggested another physical mechanism based on a Rossby-type atmospheric response to the SSTAs in the tropical *western* Pacific.

Using observations for almost 100 yr, Krishnan and Sugi (2001) statistically confirmed a year-to-year out-of-phase relationship with Indian rainfall, that is, the Indian summer monsoon. To give a physical explanation to the negative correlation, they proposed two dominant routes of teleconnection: one is the southern oceanic route from the Indian subcontinent to the western Pacific and the other is the midlatitude continental route over the Eurasian continent. Yet, further verification is needed to understand the robust physical mechanisms whereby the baiu phenomenon is related to the ENSO and to the interannual variations of the Asian summer monsoon. In particular, the physical linkage to the biennial oscillation (BO) dominating the Asian–Australian monsoon (Meehl 1987; Tomita and Yasunari 1996; Li and Zhang 2002) is still unclear.

This study first reveals the interannual variations of the baiu front, particularly, focusing on the meridional fluctuation in the western North Pacific. Then, the influence of large-scale circulations on the interannual variability is examined with specific emphasis on the effects from the Tropics. The physical mechanisms are discussed with the interannual ENSO and with the tropical BO of the Asian–Australian monsoon. Since the amplitude tends to reach its maximum in boreal winter of both the BO and ENSO, the physical processes are examined from northern winter to early summer. The findings derived from this study will contribute to raising the predictability of the baiu phenomenon and enhance the physical understanding of interannual variability prevailing in the early summer climate in the western North Pacific.

In the remaining sections of this paper, section 2 introduces the employed datasets and analysis procedures. Section 3 exhibits the dominant meridional fluctuations of the baiu front on interannual time scales. The concurrent large-scale circulations and the time development from the preceding winter to early summer are examined in section 4. Section 5 gives a summary and further discussion. Note that seasons in the text correspond to those in the Northern Hemisphere unless otherwise noted.

2. Data and analysis procedures

In this work, the following three datasets were used: 1) global precipitation estimated in the Climate Prediction Center (CPC) Merged Analysis of Precipitation (CMAP; Xie and Arkin 1996, 1997); 2) atmospheric parameters assimilated in the National Centers for Environmental Prediction–National Center for Atmospheric Research (NCEP–NCAR) reanalysis (Kalnay et al. 1996); and 3) observational global ice and SST (GISST) compiled at the Met Office (Rayner et al. 1996). The SST data without sufficient observations were reconstructed by a linear sum of covariance empirical orthogonal functions (EOFs) weighted by the correspondingly adjusted time coefficients (Parker et al. 1995). The three datasets had no missing data, and the data were all arrayed on grids covering the entire globe at 1.0° or 2.5° intervals. Since our strategy was to exhibit significant variations on interannual time scales, time resolution in months was employed for the periods of 1979–2000 (22 yr) for CMAP and 1979–99 (21 yr) for GISST and NCEP–NCAR reanalysis. In order to examine the phase relationship with the interannual ENSO and Indian summer monsoon variations, we further employed the monthly Southern Oscillation index (SOI) defined by the sea level pressure difference between Tahiti and Darwin (Tahiti − Darwin) and the monthly all-India rainfall updated by the Indian Institute of Tropical Meteorology (Parthasarathy et al. 1995).

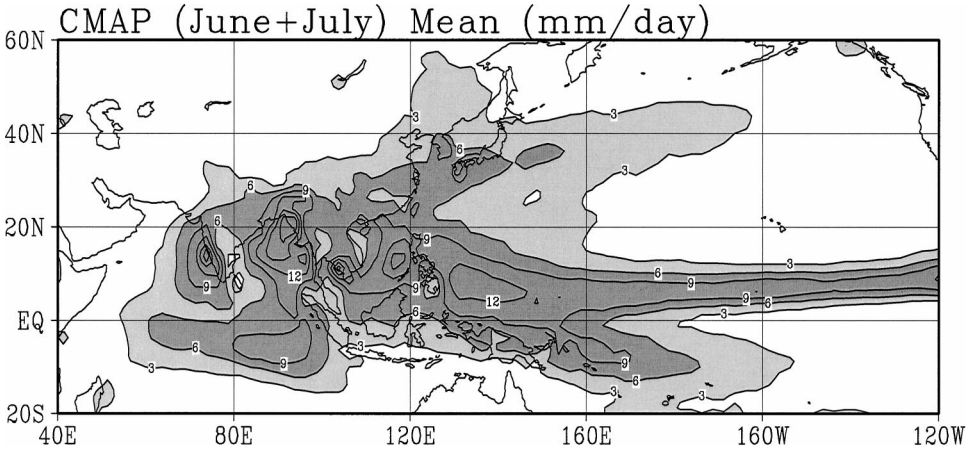

FIG. 1. Long-term (1979–2000) Jun–Jul precipitation mean. The contour interval is 3 mm day^{-1}, and regions with values larger than 3 (6) mm day^{-1} are lightly (darkly) shaded.

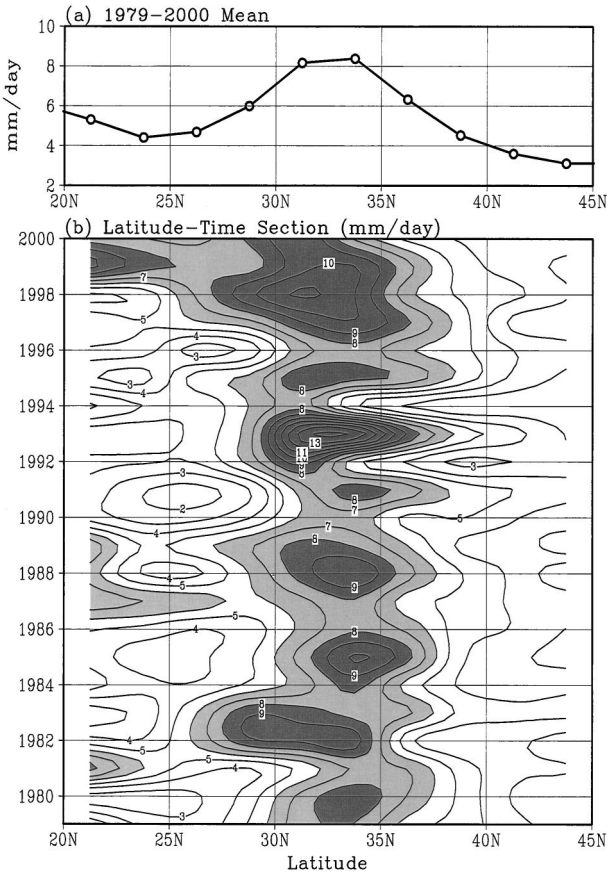

FIG. 2. Meridional section at 130°–140°E of the Jun–Jul precipitation mean: (a) the long-term (1979–2000) mean and (b) the real interannual variation for 1979–2000. The contour interval is 1 mm day^{-1} in (b), and regions with values larger than 6 (8) mm day^{-1} are lightly (darkly) shaded.

In order to extract dominant spatial patterns that may be involved in a spatiotemporal dataset, we applied EOF analysis for the spatial covariance matrix estimated in the time direction. In addition, the periodicity of the EOF time coefficients was examined using power spectral analysis. The composite and lag-correlation techniques based on the EOF time coefficients are usable to demonstrate the spatial patterns reflecting each of the EOF modes on any anomaly fields. The significance of the anomalies and correlations was statistically estimated by the two-tailed Student's *t* test.

3. Meridional variation of the baiu front on interannual time scales

The baiu precipitation near Japan is distinguished from the main body of the Asian monsoon at a glance (Fig. 1). The humidity advection from the south encounters the cold advection from the north in the midlatitudes near Japan and results in large baroclinicity there, that is, the baiu front (Ninomiya 2000). It is, therefore, conceivable that the meridional fluctuation of the baiu front sensitively reflects the large-scale meridional circulations in the western Pacific. As representative longitudes we set 130°–140°E.

The interannual variation of the baiu front is identified not only in strength but also in spatial location. Figure 2a illustrates the long-term (1979–2000) mean of the meridional rainfall distribution averaged during the baiu season (June and July) in the 130°–140°E longitude strip. The baiu front is climatologically located at 30°–35°N near Japan, as indicated by the local maximum (Figs. 1 and 2a). The interannual fluctuation is, however, large in both amplitude and meridional distribution, as shown in Fig. 2b. For instance, during the last two decades, the baiu has experienced its largest and smallest precipitation in 1993 and 1994, respectively, within a year. Moreover, the baiu front extended far south in 1982 and 1983. It is ascertained from Fig. 2b that the fluc-

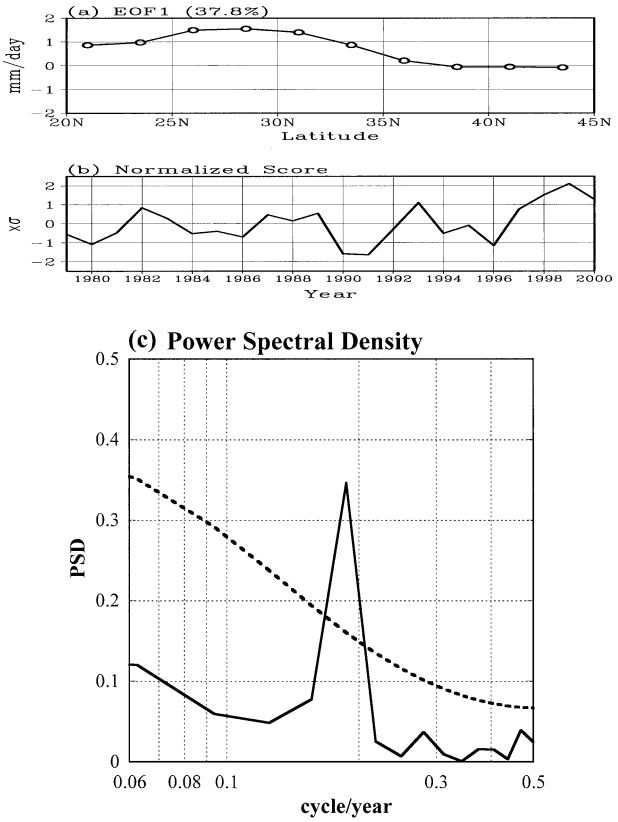

FIG. 3. (a) First EOF interannual fluctuation of Jun–Jul precipitation mean averaged in the 130°–140°E longitude strip (Fig. 2b) and (b) time coefficients. The time coefficients are normalized, while the standard deviation is imposed on the EOF. (c) Power spectral density (PSD) of the normalized time coefficients (solid line) with 95% significance (dotted line) based on the red noise spectrum estimated from a first-order autoregression.

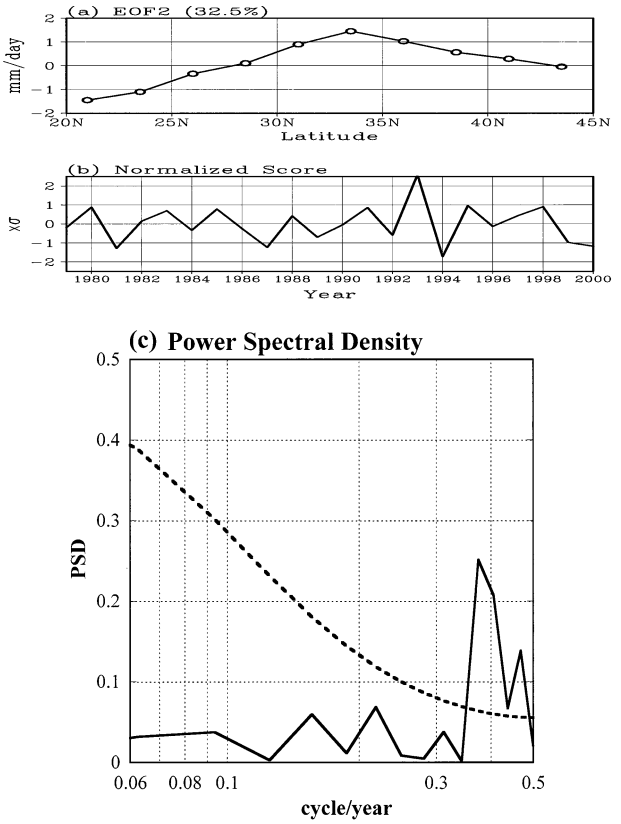

FIG. 4. As in Fig. 3 but for the second EOF.

tuations occurred quasi biennially, which further suggests that the variability is synchronized with the biennial modulation of the Asian–Australian monsoon (cf. Meehl 1987; Tomita and Yasunari 1996; Li and Zhang 2002). At latitudes south of 30°N, the biennial fluctuation seems to be less dominant than the interannual variation with a longer period of 5 or 6 yr.

In order to extract the dominant interannual variations that are indicated in Fig. 2b, we applied the EOF analysis to a time–latitude dataset. Figures 3 and 4 exhibit the first and second EOFs, respectively, and the corresponding normalized time coefficients, where the standard deviations are imposed on the respective EOFs. The contribution rates to the total variance of the first two EOF modes are 37.8% and 32.5%, respectively, and total over 70%, while that of the third EOF mode is 17.8%. Since a propagating feature is usually explained by two EOF modes with almost equal contribution rates but with a quadrature phase difference in time, we additionally inspected the periodicity of the time coefficients (Figs. 3c and 4c). A power spectrum analysis evidently demonstrates that the predominant periods are different in the two EOF modes, indicating that not only simultaneous but also lagged correlations are low between the two time coefficients. This assures that the two EOF modes are not a *pair* expressing a *propagating variation.* The almost equal contribution rates and the different periodicity suggest that there are two distinct controlling mechanisms for the interannual meridional variation of the baiu front. The present work sheds light on the mechanisms associated with the two leading EOF modes.

The first EOF mode (Fig. 3) manifests a standing oscillation to the south of 35°N with a period of 5 or 6 yr. In the spatial pattern (Fig. 3a), a positive maximum appears in the 25°–32°N latitudinal band to the south of 35°N. The temporal variation (Fig. 3b) indicates the dominance of a 5- or 6-yr period (Fig. 3c), and the years of positive maximum are well synchronized with warm ENSO events, that is, 1982–83, 1987–88, 1992–93, and 1997–98. In fact, the simultaneous correlation of time coefficients with the SOI is −0.47, significant at the 5% level (0.37). In other words, the baiu precipitation tends to be large in early summers after the warm ENSO events, as Zhang et al. (1996) and Tanaka (1997) have pointed out. Contrary to the findings of Krishnan and Sugi (2001), however, the concurrent correlation with the all-India rainfall is −0.19, insignificant at the 5% level.

TABLE 1. List of composite years (1900 is subtracted).

LF (+)	82	83	87	88	89	93	97	98	99			
LF (−)	79	80	81	84	85	86	90	91	92	94	95	96
BO (+)	80	82	83	85	88	91	93	95	97	98		
BO (−)	79	81	84	86	87	89	90	92	94	96	99	

The second EOF mode (Fig. 4) specifies a seesawlike variation with a node at around 28°N fluctuating quasi biennially. The period is definitely shorter than the 5- or 6-yr period of the first EOF mode (cf. Fig. 4c with Fig. 3c). The quasi-biennial fluctuation represents a variation at 30°–35°N, shown in Fig. 2b. Hereafter, the first EOF mode is referred to as the lower-frequency (LF) mode, while the second EOF mode is referred to as the biennial oscillation (BO) mode. The original time variation is well explained by the spatiotemporal phase of the LF and BO modes, as identified in Fig. 2b. For instance, the largest baiu event of 1993 corresponded to the largest positive maximum of the BO mode (Fig. 4b) and to the moderate positive maximum of the LF mode (Fig. 3b). In contrast, the phase was opposite in 1999, when the largest positive maximum appeared in the LF mode (Figs. 3b and 4b). In that year, the baiu front largely expanded southward without a node around 28°N (Fig. 2b). Unlike those of the LF mode, the time coefficients of the BO mode are not significantly correlated with either the SOI (−0.09) or the all-India rainfall (0.13). Correlations with the ENSO or with the Indian summer monsoon will be considered in greater detail in the following sections, which examine the accompanying spatial patterns in anomaly fields.

4. Large-scale circulations associated with the LF and BO modes

Spatial anomaly distributions of atmospheric parameters were examined to determine significant differences between the interannual LF and BO modes. This section particularly focuses on the large-scale circulations surrounding the baiu front, ENSO, and the Asian summer monsoon. To exhibit the differences clearly, we employed composite and lag-correlation techniques based on the EOF time coefficients for each mode (Figs. 3b and 4b). The composite years are chosen by signs listed in Table 1. The anomalies are defined by subtracting the mean of the negative years from that of the positive ones, and the significance of the anomaly is tested by applying the two-tailed Student's *t* test to the difference of two sample means. The lag correlations are also tested by a similar *t* statistic.

a. Circulation fields in the baiu season

Precipitation in the Tropics, which is also a proxy indicator of latent heating, can expose an anomalous convection. Figure 5 shows the anomaly fields when the baiu rainfall is large near Japan, as associated with the LF and BO modes. In both the LF and BO fields, distinct positive anomalies extend from the East China Sea to the east zonally. Parallel positive and negative anomalies appearing in the tropical central–eastern North Pacific are also common in the two fields, although the anomalies are somewhat smaller in the BO field (Fig. 5b). The parallel pattern reflects the intertropical convergence zone that anomalously shifts equatorward,

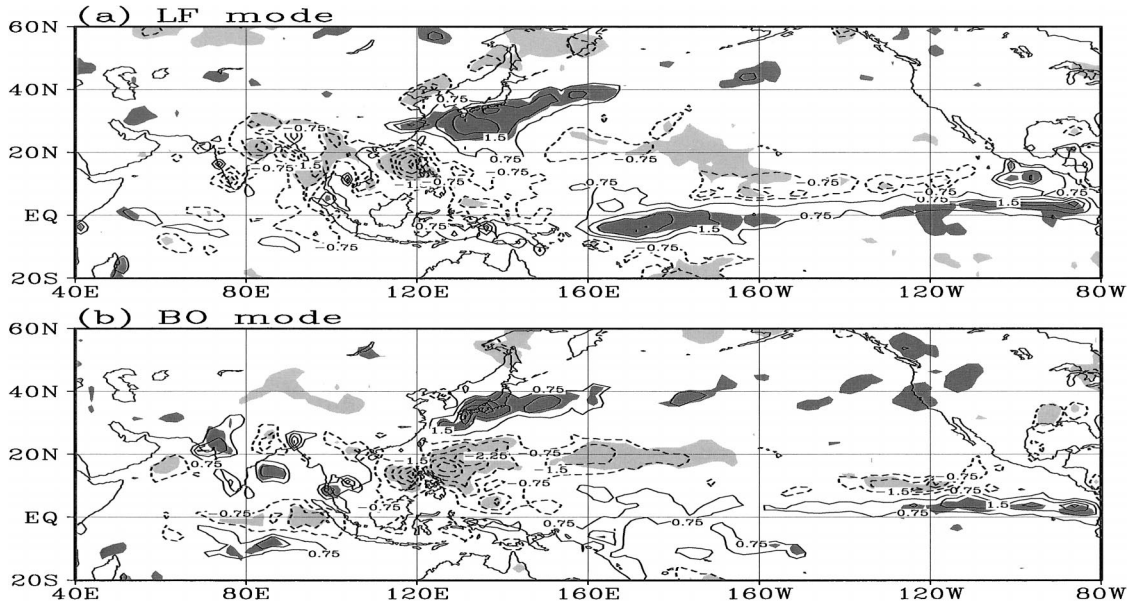

FIG. 5. Composite precipitation anomalies based on the first (LF) and second (BO) EOF time coefficients (Table 1) (a) for the LF mode and (b) for the BO mode. The contour interval is 0.75 mm day^{-1}. Dotted lines indicate negative contours, while zero lines are omitted for clarity. Regions being positively (negatively) significant at 5% are darkly (lightly) shaded.

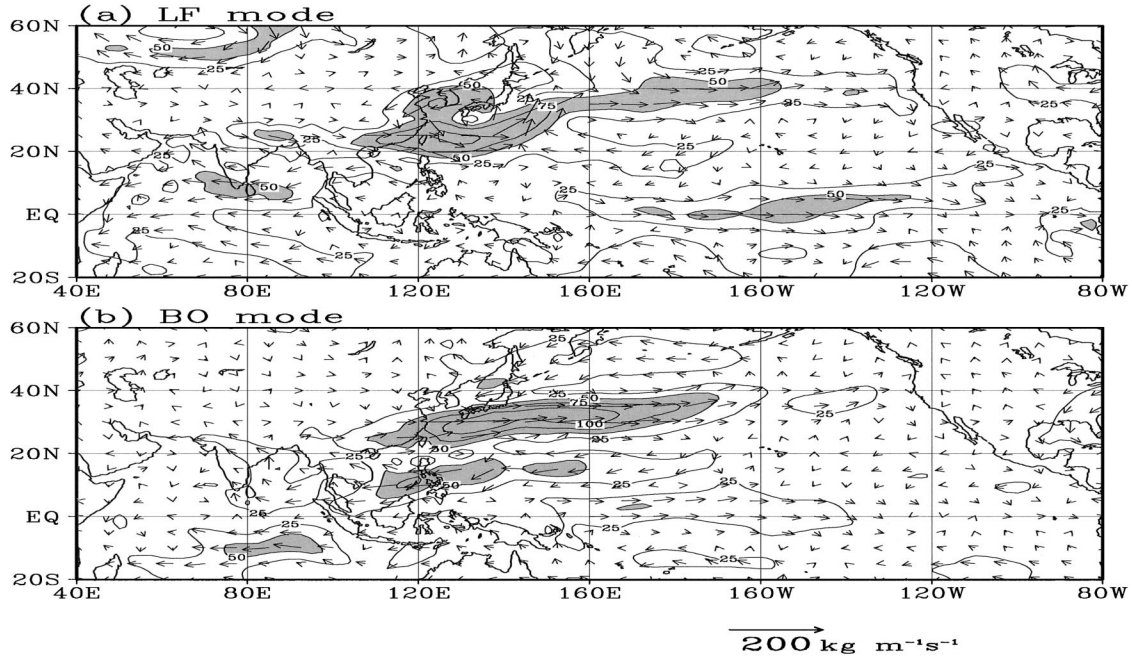

FIG. 6. Anomaly vectors of vertically integrated water vapor flux based on the (a) LF and (b) BO EOF time coefficients (Table 1). The reference vector of the two is exhibited in common near the bottom of (b). Contours indicate the size of the vector at an interval of 25 kg m^{-1} s^{-1}; regions larger than 50 kg m^{-1} s^{-1} are shaded.

which is typical when an ENSO event appears (e.g., Wallace et al. 1998).

In the western North Pacific, the Pacific–Japan (PJ)-like pattern (Nitta 1987, 1989) is discernible in the two fields, that is, an anomalously weak convection around the Philippines and a strong one to the north that results in larger-than-normal baiu precipitation near Japan. In the BO mode (Fig. 5b), the meridional contrast in anomaly well reflects the seesawlike fluctuation of the baiu front (Fig. 4a), whereas the anomalous southward expansion of the baiu front (Fig. 3a) is certainly notable near Japan in the LF mode (Fig. 5a). In addition, we can identify distinct spatial differences in the large-scale zonal distribution of negative anomalies around the Philippines. The negative anomalies extend westward from the South China Sea (SCS) to the Indian subcontinent in the LF field (Fig. 5a) but eastward from the SCS to the TWNP in the BO field (Fig. 5b). The zonal differences of the anomalous convection along 20°N, that is, east or west of 120°E, correspond to the predominant mode. Therefore, the BO mode is negatively correlated with the TWNP monsoon, the LF mode, and with the south-southeast Asian (SSEA) monsoon, although there are some areas with insignificant negative anomalies in the Indian subcontinent. Such differences favorably adjust the anomalous distribution of the baiu front through the modification of meridional circulations in the western North Pacific, which will be further examined in a later subsection. Similar results can also be derived by examining the outgoing longwave radiation instead of the precipitation (not shown).

The vertically integrated water vapor flux in the troposphere is a useful parameter to trace the moisture following large-scale circulations. In order to determine the relative differences between the LF and BO modes, we examined the vectors defined as follows:

$$\mathbf{Q} \equiv \frac{1}{g}\int_{300\ \mathrm{hPa}}^{1000\ \mathrm{hPa}} \mathbf{v}q\ dp,$$

where g is the acceleration of gravity, $\mathbf{v}$ is a horizontal wind vector, and q is specific humidity that is quite small and negligible above 300 hPa.

Figure 6 illustrates the distributions of anomalous $\mathbf{Q}$ when the baiu precipitation is large near Japan, as associated with the LF and BO modes. When the LF mode is dominant (Fig. 6a), the region with large eastward $\mathbf{Q}$ ($|\mathbf{Q}| > 50$ kg m^{-1} s^{-1}) extends from the East China Sea to the central North Pacific zonally. A large-scale cyclonic circulation with its center located in the south of Japan is superimposed on the western part of the region. The cyclonic circulation with a southward meander corresponds to the anomalous southward expansion of the baiu front that characterizes the LF mode (Figs. 3a and 5a). Additionally, two other large $\mathbf{Q}$ regions are observed in the Indian Ocean and the equatorial central Pacific. The latter, with an easterly direction, supports the idea that the LF mode is closely related to ENSO, while the former, with a westerly direction, indicates that the SSEA monsoon is weak when the LF mode is prominent.

The region with large eastward $\mathbf{Q}$ is more zonal near

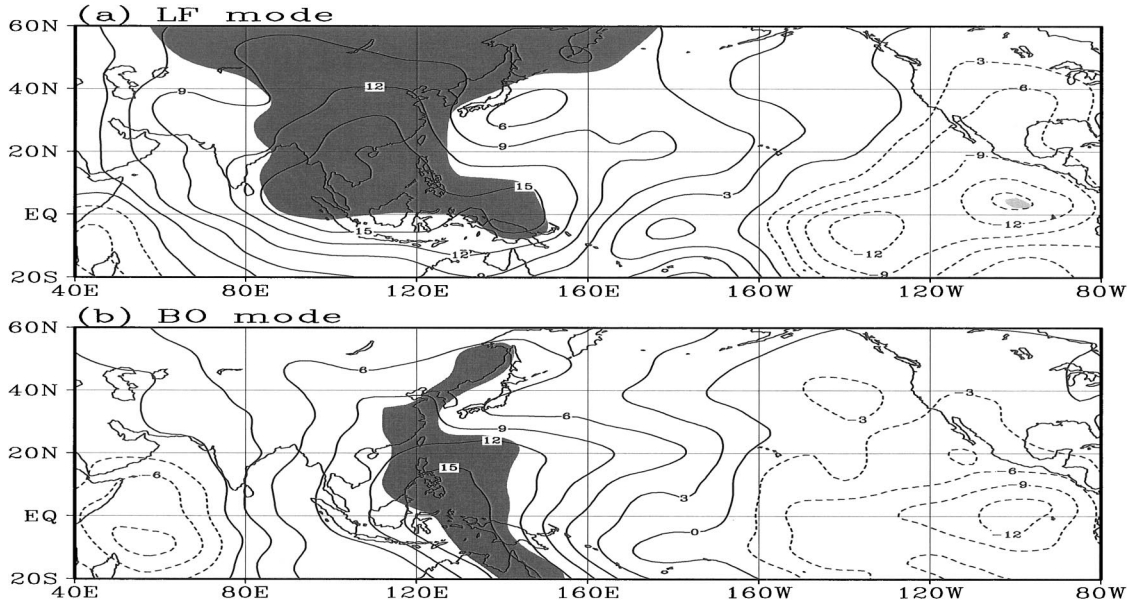

FIG. 7. Composite anomalies of the velocity potential at 200 hPa based on the (a) LF and (b) BO EOF time coefficients (Table 1). The positive anomalies are set to anomalous convergence. The contour interval is 3×10^5 m^2 s^{-1}, and the dotted lines indicate negative values. Significance is tested using the Student's *t* test, and regions with dark (light) shading are positively (negatively) significant at 5%.

Japan when the BO mode is predominant, which again extends from the eastern part of the Asian continent to the central North Pacific (Fig. 6b). The anomalous baiu precipitation characterizing the BO mode (Figs. 4a and 5b) is attributed to the convergence of **Q** near Japan that is estimated from vectors with opposite directions straddling the 35°N latitude. Furthermore, there is a region with large easterly **Q** in the TWNP south of 20°N, which implies stronger-than-normal trade winds. A large-scale anticyclone is formed along 20°N in the TWNP between two large **Q** regions with opposite zonal directions, where the precipitation anomalies are certainly negative (Fig. 5b). Besides the two large **Q** belts aforementioned, regions with relatively large **Q** can be identified in the equatorial central Pacific and to the north of Japan. The equatorial vectors are placed between 160°E and 160°W to the west of the region shown in the LF mode (Fig. 6a), about 30° longitude. The four large **Q** belts extending northward in the western North Pacific with alternate zonal directions are reminiscent of the PJ pattern found by Nitta (1987, 1989).

When the LF mode is dominant, large **Q** regions appear broadly in the Pacific–Indian Ocean sector (Fig. 6a), whereas four large **Q** belts are confined to narrower longitudes in the central–western North Pacific when the BO mode prevails (Fig. 6b). The LF mode is characterized by a global structure consistent with the warm ENSO event and with the weak SSEA monsoon, while the structure of the BO mode is less global and is locally synchronized with the TWNP monsoon.

In order to further identify the large-scale circulations associated with each of the LF and BO modes, we examined the velocity potential at the 200-hPa level (φ_{200}) using similar composite analysis (Fig. 7). Note that the positive φ_{200} corresponds to convergence, as defined by $\nabla\varphi = (u, v)$, where u and v are the zonal and meridional components of horizontal winds, respectively. As a common feature, we identify a large positive/negative difference between the Indonesian Maritime Continent and the tropical eastern Pacific, implying a weaker-than-normal Walker circulation. The positive anomalies around the Maritime Continent correspond well to the negative anomalies in precipitation (Fig. 5). In general, the Asian summer monsoon is weak when either mode is largely positive.

Differences between the two modes have also been identified. When the LF mode is dominant (Fig. 7a), the positive anomalies extend broadly in the Asian monsoon region where the maximum axis of the positive anomalies inclines from the northwest to the southeast. At longitudes between 120° and 160°E, the local maximum and minimum appear around the equator and near Japan, respectively, reflecting the weaker-than-normal Hadley circulation in the western North Pacific. The locally weak Pacific high allows the baiu front to expand southward and bring more precipitation near Japan (Figs. 3a and 5a).

On the other hand, when the BO mode is prominent (Fig. 7b), the region with positive anomalies is confined to the western Pacific where the axis of the positive maximum is meridional and the significant signals are to the east of 120°E. At longitudes of 120°–160°E, the four local maxima/minima are identified at around 5°S, 20°N, and 35°N near Japan and at 50°N, where the positive maximum along 20°N is the most noteworthy. The structure of the BO mode, which differs from the larger

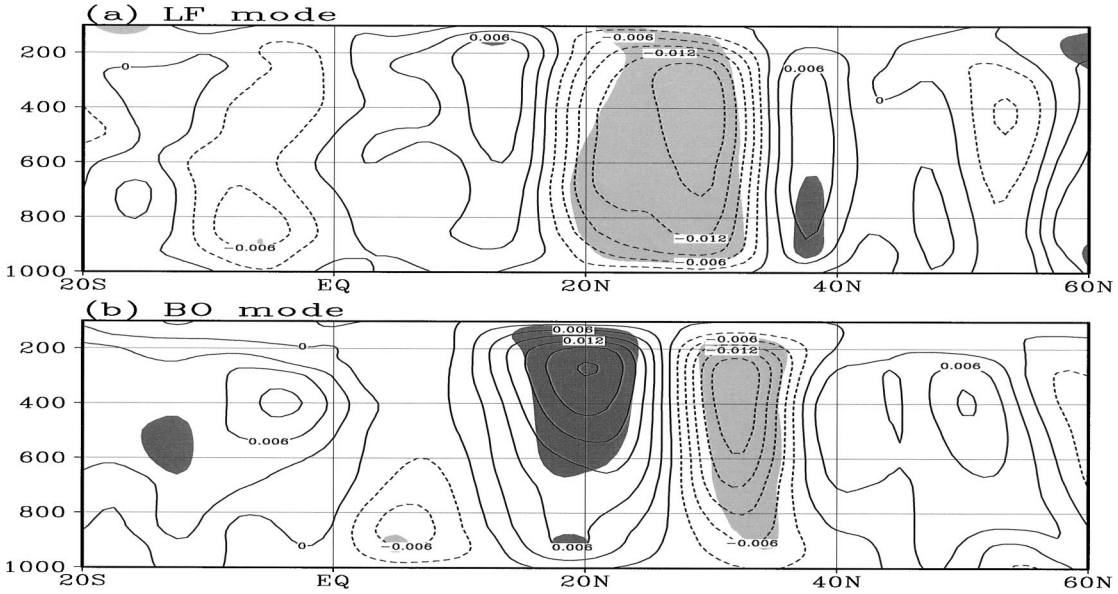

FIG. 8. Latitude–height sections of vertical *p*-velocity anomalies (Pa s^{-1}) averaged in the 130°–140°E longitude strip in June and July associated with the (a) LF and (b) BO modes (Table 1). The contour interval is 0.003 Pa s^{-1}, and the dotted lines indicate negative (upward) values. Significance is tested using the Student's *t* test, and regions with dark (light) shading are positively (negatively) significant at 5%.

one-cell structure of the LF mode, consists of three cells of anomalous meridional circulation in the western Pacific. The local minimum around Japan and the maximum along 20°N correspond to a southward shift of the Pacific high in the western North Pacific and reflect a seesawlike fluctuation of the baiu precipitation in the BO mode (Figs. 4a and 5b). The spatial scale of the circulations is smaller in both zonal and meridional directions in the BO mode than in the LF mode.

In order to specify the meridional modulation of the Hadley circulation and the anomalous zonal circulations associated with the LF and BO modes, which reflect the deformation of the subtropical Pacific high, we examined a latitude–height section of the anomalies of the vertical *p* velocity in the TWNP (130°–140°E) (Fig. 8). Then, we investigated the longitude–height section along 20°N (15°–25°N) (Fig. 9) where zonal differences are significant in a precipitation field (Fig. 5).

When the LF mode is dominant (Fig. 8a), anomalous upward flows are significant in 20°–35°N where the baiu

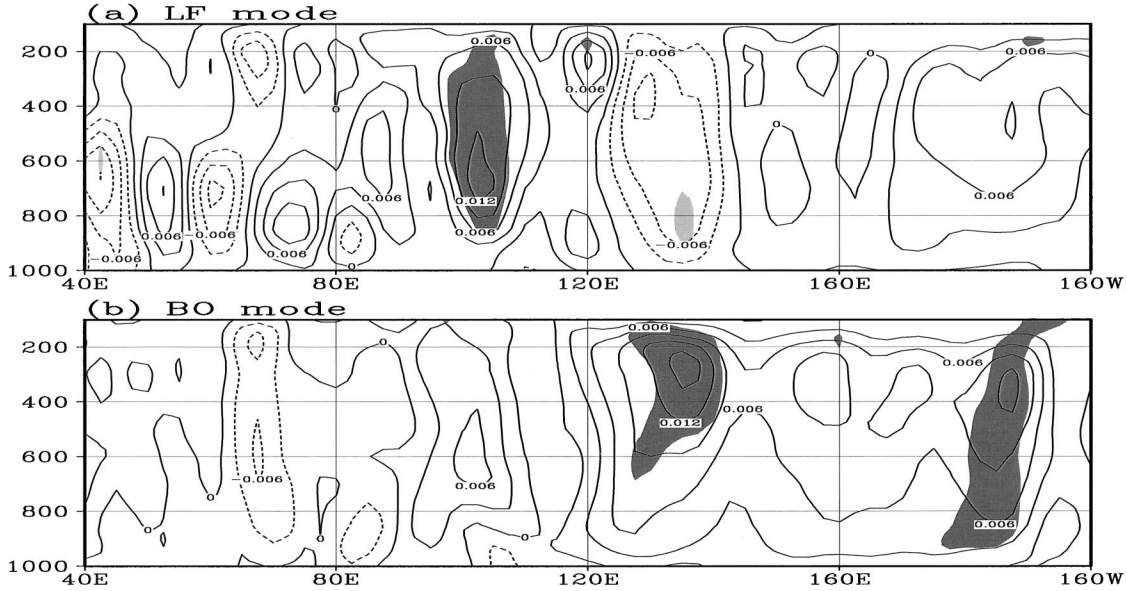

FIG. 9. As in Fig. 8 but averaged in the 15°–25°N latitude strip.

front expands southward anomalously (Figs. 3a and 5a). This indicates a relatively weak Pacific high in the western part. An ascent is also detectable about 5°S of the equator, while a compensative descent appears in the region between the equator and 15°N, implying that the Hadley circulation is anomalously modified in the TWNP. As suggested earlier, the LF mode is characterized by a large-scale anomalous meridional circulation centered at around 20°N between 5° and 35°N. There is also a significant descent in the lower troposphere to the north at the narrow 35°–40°N latitudes.

When the BO mode is prominent (Fig. 8b), an anomalous descent at around 20°N and an ascent at 35°N complementarily adjust the baiu front northward (Figs. 4a and 5b). The Pacific high is strong (weak) in the southern (northern) part of the TWNP in conjunction with the BO mode dominance. The latitudes of the ascent and descent correspond to those of the positive and negative anomalies in precipitation, respectively (Fig. 5b), and reflect the seesawlike fluctuation of the baiu front with a node at around 28°N (Fig. 4a). The meridional circulation characterizing the BO mode, that is, the anomalous ascent and descent between 15° and 35°N, is located about 5° to the north of those in the LF mode. Furthermore, the distance between the descending and ascending axes, that is, 20° and 35°N (Fig. 8b), is narrower than that between the 10° and 30°N of the LF mode (Fig. 8a), indicating that the scale of anomalous meridional circulation is smaller in the BO mode than in the LF mode, as shown in Fig. 7. The ascent near 5°N (Fig. 8b) does not seem to reflect the positive precipitation anomalies (Fig. 5b) because of the weak convection with a height lower than 600 hPa. Between the equator and 40°N, the branches of the anomalous ascent and descent in the BO mode are placed in the quadrature phases of those of the LF mode. The differences in meridional circulations are essential to the meridional modulation of the baiu front.

In order to investigate the zonal differences along 20°N shown in Figs. 5, 6, and 7, we examined the anomalous zonal circulations associated with each mode, which further diagnosed details of the relationship with the Asian summer monsoon (Fig. 9). As found in Fig. 8, significant differences are identified in the anomalies of the vertical p velocity at 130°–140°E; that is, it is upward in the LF mode (Fig. 9a) but downward in the BO mode (Fig. 9b). Moreover, we observed a significant anomalous descent around 100°E in the LF mode (Fig. 9a), indicating that the SSEA monsoon is weak when the baiu activity is strong with this mode (see also Fig. 5a). The negative correlation between the baiu activity and the SSEA monsoon is consistent with the findings of Tanaka (1997). On the other hand, when the baiu precipitation is large with the BO mode (Fig. 9b), a significant descent appears to the east of 120°E in the western North Pacific, reflecting the weak TWNP monsoon (see also Fig. 5b). The broad expansion of the positive anomalies to the east of 120°E corresponds well to the negative anomalies in precipitation (Fig. 5b), indicating that the Pacific high is relatively strong in the southern or southwestern part. The correlation between the Asian monsoon and the baiu precipitation near Japan is locally modified according to the dominant mode, that is, the SSEA monsoon with the LF mode and the TWNP monsoon with the BO mode.

b. Development of the LF and BO modes from winter

Tomita and Yasunari (1993) pointed out that the El Niño events are classified into two categories according to duration: a single winter BO event and a two-consecutive-year LF event. The significant differences of the two appear in the low-level atmospheric circulation off the Philippines, especially in the recessive stage from winter to spring. However, these researchers did not examine the possibly large influence in the following baiu season. Using the lag-correlation technique based on the EOF time coefficients (Figs. 3b and 4b), this subsection examines the physical process from winter to summer that causes the development of the two interannual modes of the baiu front. The significance of the lag-correlations is judged through the two-tailed Student's t test.

Figure 10 shows the lag correlations in precipitation within the 2-month mean fields aligned from winter to early summer. In the winter preceding the LF mode development (Fig. 10a), weak positive correlations, which approach Japan when strengthened by the following seasons (Figs. 10c and 10e), are placed to the southeast of Japan with an axis from the southwest to northeast. Concurrently, a pair of regions with significant positive and negative correlations moves westward in the tropical Pacific. The resulting spatial pattern is shown in Fig. 5a. The development of the LF mode seems to be synchronized with the retreat of the ENSO event, as can be demonstrated by two facts: First, the correlation pattern in the tropical Pacific, that is, the positive correlations in the equatorial Pacific and the negative ones to the north, is typical when the ENSO events occur. Second, the pair of anomalies moves westward from winter to summer slowly (Lau and Sheu 1988; Tomita 2000). It should be noted that, in the progression, no significant correlations appear along 20°N in the TWNP.

On the other hand, in seasons proceeding to the BO mode development (Figs. 10b,d,f), regions with significant negative correlations tend to appear around the TWNP through Southeast Asia, from where they move westward along the 20°N latitude during the seasons. Since no significant correlations appear in the tropical eastern Pacific, this clearly implies that the BO mode is less related to the ENSO than the LF mode. In a theoretical study using a simple five-box model, Chang and Li (2000) pointed out that the BO of the Asian–Australian monsoon is driven by the anomalous convection around the Indonesian Maritime Continent and

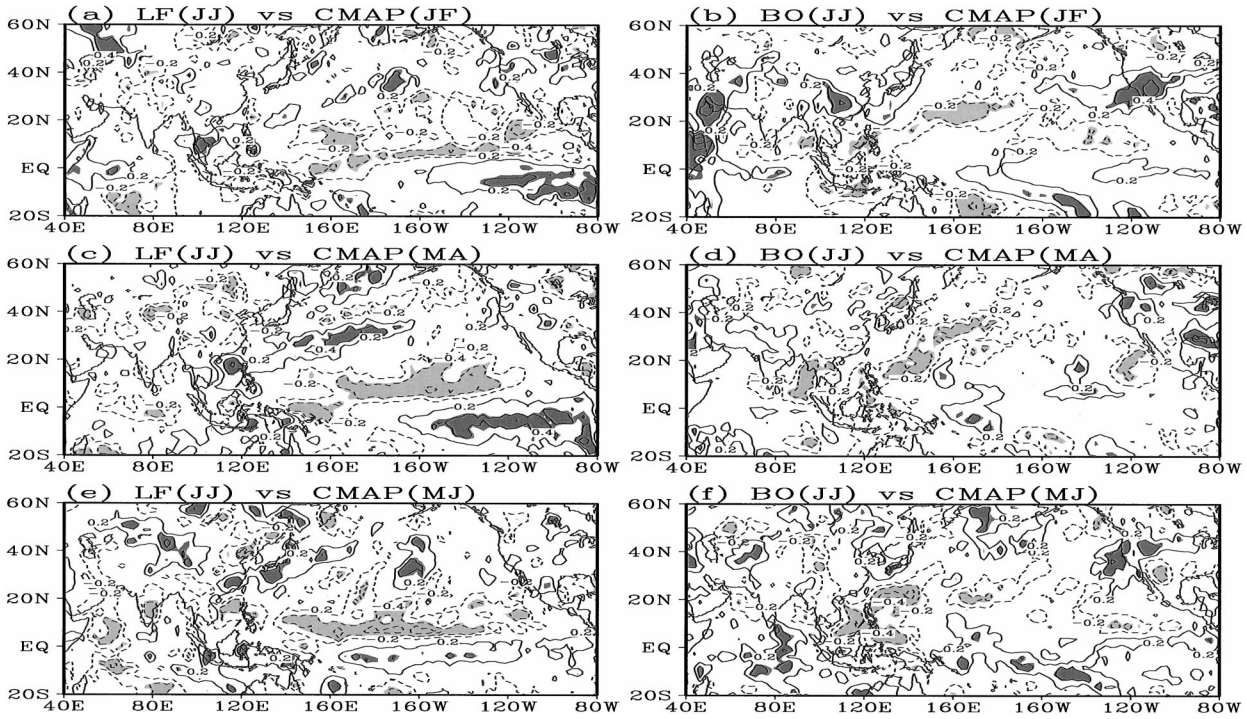

FIG. 10. Lag-correlations of precipitation estimated with the EOF time coefficients for the (left) LF and (right) BO modes. The letters JF, MA, MJ, and JJ indicate Jan–Feb, Mar–Apr, May–Jun, and Jun–Jul. The contour interval is 0.2, and the dotted lines indicate negative correlations. Significance is tested using the two-tailed Student's *t* test, and the darkly (lightly) shaded areas indicate positively (negatively) significant correlations at the 5% level (± 0.37). For brevity, the zero lines are omitted.

that the signals are weak in the tropical eastern Pacific. The findings of this study are consistent with their results. As shown in Figs. 5a and 5b, the meridional distribution of positive/negative correlations in the TWNP is different between the two modes in early summer (Figs. 10e and 10f). In other words, positive correlations extend farther south of Japan in the LF mode (Fig. 10e), while they are confined over Japan in the BO mode (Fig. 10f).

In order to determine the surface thermal conditions associated with the two baiu modes, we examined a SST field again using a similar lag-correlation technique (Fig. 11). As expected, a pronounced horseshoe pattern was identified in the entire tropical Pacific prior to the LF mode development (Figs. 11a,c,e), although the easternmost correlations expanded somewhat off the equator. The horseshoe pattern consists of positive correlations to the south of Japan and in the tropical eastern Pacific and of negative ones in between. The positive correlations to the south of Japan remain significant throughout the seasons from winter to early summer (Figs. 11a,c,e). The negative correlations in the central equatorial Pacific move westward about 10° longitude from winter to spring (Figs. 11a and 11c) as the positive ones expand westward in the equatorial eastern Pacific, consistent with the westward movement identified in the precipitation field (Figs. 10a and 10c). Significant negative correlations can also be found in the eastern North Pacific off the western coast of North America, which may be considered as a response to the atmospheric Pacific–North American pattern prevailing when the ENSO event occurs (Wallace and Gutzler 1981). In general, the correlations extending over the entire Pacific become weak as the seasons progress.

It is of interest that a horseshoe pattern is also identified in the seasons prior to the BO mode development (Figs. 11b,d,f). The pattern is, however, not well organized in the tropical eastern Pacific but advances to the tropical central–western Pacific. In addition, the spatial phase is clearly different from that of the LF mode. In other words, in the tropical Pacific, the negative and positive correlations in the BO mode (Figs. 11b,d,f) extend in regions near the zero lines in the LF mode (Figs. 11a,c,e), suggesting a quadrature phase difference in space. In the BO mode development (Figs. 11b,d,f), the significant negative correlations move westward in the TWNP off the Philippines without distinct positive ones near Japan. Furthermore, the finding that there are no significant correlations in the equatorial eastern Pacific again supports the idea that the BO mode is less related to the ENSO. The differences between the LF and BO modes are attributed to the spatial phase of horseshoe SSTAs in the tropical Pacific.

Wang et al. (2000) suggested that the ENSO can affect the following summer monsoon in East Asia through a specific teleconnection with horseshoe SSTAs in the

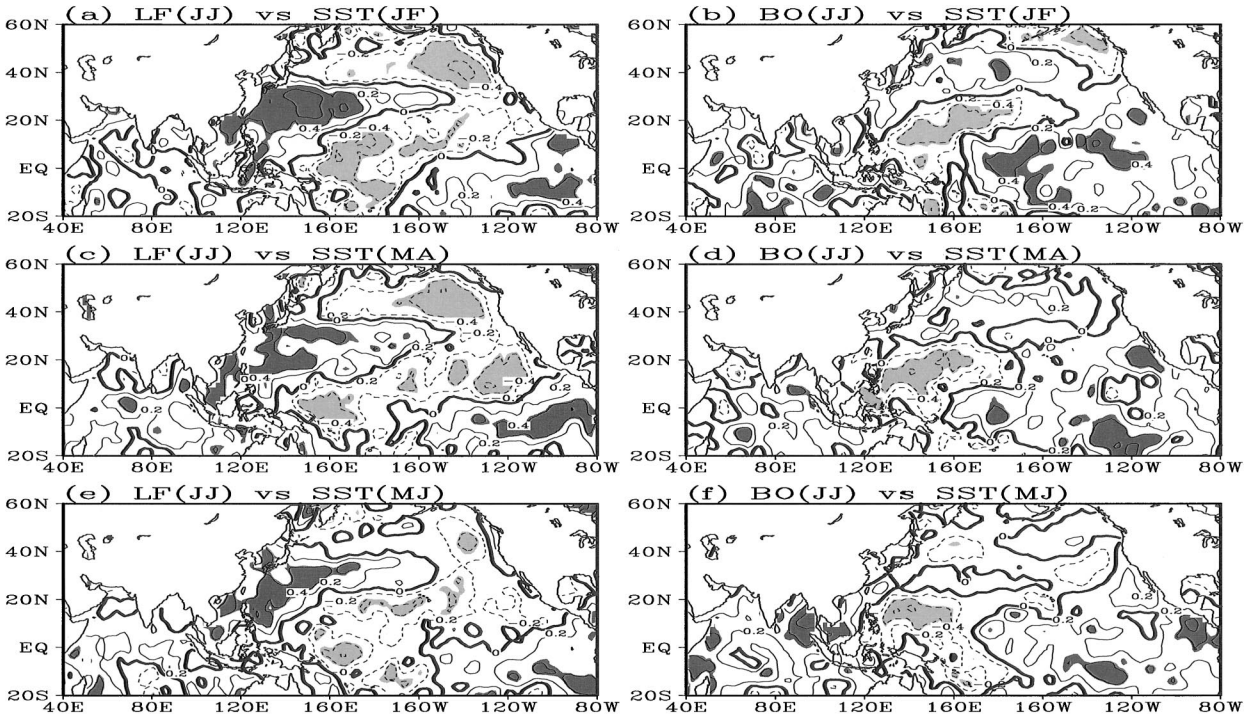

FIG. 11. As in Fig. 10 but for lag correlations of SST with thick zero lines.

tropical Pacific. The present study further points out that the BO is also related to the Asian summer monsoon through the horseshoe SSTAs but with a different spatial phase of about 90°. It is conceivable that the differences in the spatial phase modify the anomalous meridional circulations through the SSTAs in the TWNP, particularly off the Philippines, since the mean SST in the range of 28°–29°C is sensitive to the development of organization of the convection (Graham and Barnett 1987; Lau et al. 1997). In fact, the negative and positive SSTAs in the TWNP correspond well to the descent at around 20°N in the BO mode and the ascent at 20°–35°N in the LF mode (Fig. 8). Modified meridional circulations in turn control the anomalous meridional expansion of the baiu front that characterizes the LF and BO modes. The SSTAs off the Philippines may also control the zonal contrast of Asian summer monsoons through anomalous zonal circulation, that is, the correlations between the two baiu modes and the SSEA or TWNP monsoons, although, in the BO mode, the anomalous dipole straddling 120°E along the 20°N latitude is not significant in the vertical *p*-velocity field (Fig. 9).

5. Summary

The baiu (mei-yu or changma) phenomenon is one of the dominant features characterizing early summer climate in the western North Pacific. The baiu front, which advances northeastward from the southeastern foot of the Tibetan Plateau to the central North Pacific along the western periphery of the subtropical Pacific high (Fig. 1), demonstrates distinct interannual variability that significantly affects the water resources in East Asia. Focusing on the meridional fluctuation in the western North Pacific (130°–140°E), this study has identified the interannual variability and examined the relevant large-scale circulations.

The datasets mainly used in this study are the following three: 1) the GISST compiled at the Met Office, 2) precipitation estimated in the CMAP, and 3) atmospheric parameters assimilated in the NCEP–NCAR reanalysis. These are all gridded datasets covering the entire globe in monthly time resolution for the periods of 1979–2000 (CMAP) or 1979–99 (GISST and NCEP–NCAR reanalysis). In addition, the monthly time series of SOI and all-India rainfall are employed to examine the relationship with the ENSO and with the Indian summer monsoon. The analysis techniques used include the EOF, composite, lag correlation, and power spectral analyses, the latter three being based on time coefficients derived from the former EOF analysis. The significance of the anomalies and the correlations is estimated through the two-tailed Student's *t* test.

The EOF analysis detects the spatiotemporal structure of the dominant interannual variability that is involved in the time–latitude cross section of precipitation in the western North Pacific (130°–140°E) (Fig. 2). The first EOF mode represents a standing variation to the south of 35°N with a period of 5 or 6 yr (LF mode). The periodicity implies that the LF mode is synchronized to the ENSO cycle; that is, the baiu precipitation tends to

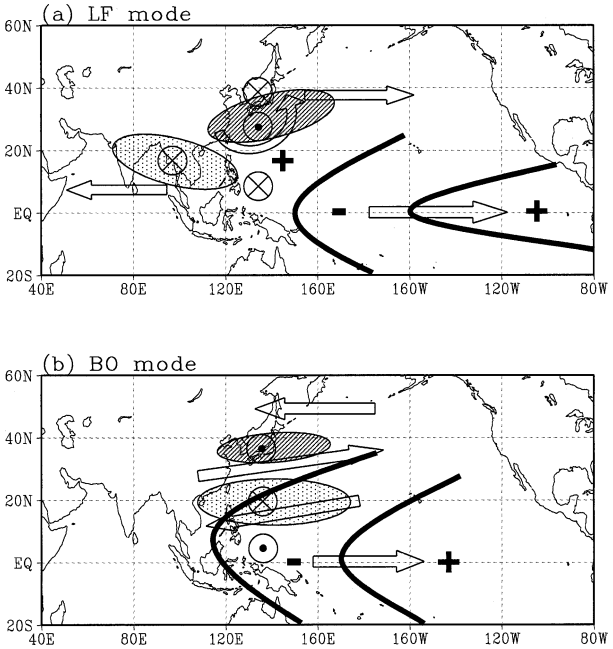

FIG. 12. Schematic diagrams illustrating the anomaly fields in early summer associated with the (a) LF and (b) BO modes. Regions with positive (negative) precipitation anomalies in the Indian Ocean–western Pacific sector are hatched (stippled) (Figs. 5 and 10), while vectors designate the location and direction of relatively large water vapor flux (Fig. 6). Circles with a dot (a cross) indicate the local centers of anomalous ascent (descent) (Figs. 8 and 9). SSTAs in the tropical Pacific are divided by thick lines with ± signs (Fig. 11).

be large after warm ENSO events. On the other hand, the second EOF mode demonstrates a seesawlike variation with a node at around 28°N fluctuating quasi biennially (BO mode). Since the contribution rates of the two EOF modes total over 70%, the composite of two modes can explain well the entire interannual variation in the meridional fluctuation of the baiu front in the western North Pacific. Although this study examines the large-scale circulations associated with the two EOF modes separately, it is, of course, necessary to compile the results to draw a more realistic picture of interannual fluctuation.

The anomalous large-scale circulations in early summer associated with the LF and BO modes are schematically summarized in Fig. 12. When the LF mode is dominant (Fig. 12a), the positive precipitation anomalies appearing along the baiu front expand southward, while the negative ones are evident in the SSEA monsoon region. The anomalies of the water vapor flux display a consistent zonal flow pattern from the East China Sea to the central North Pacific, with a southward meander that is part of a large-scale eddy to the south of Japan. The flux anomalies are also large in the equatorial central Pacific and the Indian Ocean, indicating that the LF mode is linked to the ENSO. The weaker-than-normal Walker circulation, which is estimated from the field of the velocity potential at the 200-hPa level (φ_{200}) (Fig. 7), also supports the linkage with the ENSO. The negative precipitation and positive φ_{200} anomalies around Indochina reflect the weaker-than-normal SSEA monsoon. When the LF mode is prevailing, the correlation is negative between the baiu precipitation and the SSEA monsoon. The meridional circulations characterizing the LF mode comprise branches of descent at around 10°N, ascent at 20°–30°N, and descent to the north in the western North Pacific. The anomalous zonal circulation along 20°N, centered at 120°E, is also significant in the region of the Asian summer monsoon (Fig. 9).

On the other hand, when the BO mode is dominant (Fig. 12b), the meridional contrast is significant in precipitation between the regions near Japan and off the Philippines. The baiu precipitation is negatively correlated with the TWNP monsoon but not with the SSEA. In the anomaly field of the water vapor flux, the BO mode is distinguished by four banded layers from the equator to approximately 50°N in the western North Pacific (four vectors in Fig. 12b). Since the longitudes are confined to the western North Pacific west of 160°W, the tropical BO is more localized than the conventional ENSO and may be recognized as an aborted ENSO in the tropical central–western Pacific. The φ_{200} anomalies associated with the BO mode (Fig. 7b) also indicate four local maxima/minima in the western Pacific. The branches of meridional circulations are arrayed in the order of ascent at around 5°N, descent at 20°N, and ascent at 35°N from the south in the western North Pacific and are in a quadrature phase relationship with those in the LF mode. The anomalies of vertical p velocity clearly reflect the meridional seesawlike fluctuation of the baiu front that characterizes the BO mode.

Although Nitta (1987, 1989) pointed out that the PJ pattern appeared in the western North Pacific in conjunction with the interannual variation of the baiu phenomenon, the present work further reveals that the zonal and meridional circulations are definitely different between the LF and BO modes. The LF mode has significant correlation with the ENSO and with the SSEA monsoon, and the BO mode with the TWNP monsoon. From the preceding winter, the development of the LF mode indicates the close linkage with the ENSO through the horseshoe SSTAs extending in the entire tropical Pacific. The anomalous ascent (descent) corresponds well to the positive (negative) SSTAs in the western North Pacific, which leads to the meridional modification of the baiu front that characterizes the LF mode. Although the development of the BO mode is also related to similar horseshoe SSTAs, the regions with significant SSTAs are confined to the tropical western Pacific and exhibit a quadrature phase difference in both zonal and meridional directions. Accordingly, the meridional circulations in the western North Pacific are in a quadrature phase relationship with those of the LF mode. In particular, there is a distinct difference along 20°N latitude. The meridional distribution of the SSTAs in the TWNP, which is attributed to the spatial phase of

the anomalous horseshoe pattern in the tropical Pacific, affects the distribution of the baiu front through anomalous meridional circulations. The spatial phase of SSTAs may also have a zonal effect on the strength of the Asian summer monsoon between the SSEA and the TWNP. Further study is needed to examine the processes of the interannual variability of the Asian summer monsoon and verify the effects of the ENSO and the tropical BO on the processes. Approaching how horseshoe SSTAs modify the ENSO/monsoon system would be crucial to this end.

Acknowledgments. The authors would like to thank two anonymous reviewers for their constructive comments, which were very helpful in improving the manuscript. They are also grateful to Drs. Bin Wang and Tim Li for valuable information, comments, and suggestions that enhanced the discussion. This study was supported by the Frontier Research Center for Global Change, Japan Agency for Marine-Earth Science and Technology, and by a Grant-in-Aid for Scientific Research (14740283) by the Ministry of Education, Culture, Sports, Science, and Technology (MEXT) of Japan.

REFERENCES

Chang, C.-P., and T. Li, 2000: A theory for the tropical tropospheric biennial oscillation. *J. Atmos. Sci.,* **57,** 2209–2224.

Graham, N. E., and T. P. Barnett, 1987: Sea surface temperature, surface wind divergence, and convection over tropical oceans. *Science,* **238,** 657–659.

Kalnay, E., and Coauthors, 1996: The NCEP/NCAR 40-Year Reanalysis Project. *Bull. Amer. Meteor. Soc.,* **77,** 437–431.

Kawamura, R., and T. Murakami, 1998: Baiu near Japan and its relation to summer monsoons over Southeast Asia and the western North Pacific. *J. Meteor. Soc. Japan,* **76,** 619–639.

Kawatani, Y., and M. Takahashi, 2003: Simulation of the Baiu front in a high resolution AGCM. *J. Meteor. Soc. Japan,* **81,** 113–126.

Krishnan, R., and M. Sugi, 2001: Baiu rainfall variability and associated monsoon teleconnections. *J. Meteor. Soc. Japan,* **79,** 851–860.

Lau, K.-M., and P. J. Sheu, 1988: Annual cycle, quasi-biennial oscillation, and Southern Oscillation in global precipitation. *J. Geophys. Res.,* **93,** 10 975–10 988.

——, H.-T. Wu, and S. Bony, 1997: The role of large-scale atmospheric circulation in the relationship between tropical convection and sea surface temperature. *J. Climate,* **10,** 381–392.

Lau, N.-C., and M. J. Nath, 2000: Impact of ENSO on the variability of the Asian–Australian monsoon as simulated in GCM experiments. *J. Climate,* **13,** 4287–4309.

Li, T., and Y. Zhang, 2002: Processes that determine the quasi-biennial and lower-frequency variability of the South Asian monsoon. *J. Meteor. Soc. Japan,* **80,** 1149–1163.

Meehl, G. A., 1987: The annual cycle and interannual variability in the tropical Pacific and Indian Ocean regions. *Mon. Wea. Rev.,* **115,** 27–50.

Murakami, T., and J. Matsumoto, 1994: Summer monsoon over the Asian continent and the western North Pacific. *J. Meteor. Soc. Japan,* **72,** 719–745.

Ninomiya, K., 2000: Large- and meso-α-scale characteristics of Meiyu/Baiu Front associated with intense rainfalls in 1–10 July 1991. *J. Meteor. Soc. Japan,* **78,** 141–157.

——, and H. Mizuno, 1987: Variations of Baiu precipitation over Japan in 1951–1980 and large-scale characteristics of wet and dry Baiu. *J. Meteor. Soc. Japan,* **65,** 115–127.

——, and T. Akiyama, 1992: Multi-scale features of Baiu, the summer monsoon over Japan and the East Asia. *J. Meteor. Soc. Japan,* **70,** 467–495.

Nitta, T., 1987: Convective activities in the tropical western Pacific and their impact on the Northern Hemisphere summer circulation. *J. Meteor. Soc. Japan,* **65,** 373–390.

——, 1989: Global features of the Pacific–Japan oscillation. *Meteor. Atmos. Phys.,* **41,** 5–12.

Parker, D. E., C. K. Folland, and M. Jackson, 1995: Marine surface temperature: Observed variations and data requirements. *Climate Change,* **31,** 559–600.

Parthasarathy, B., A. A. Munot, and D. R. Kothawale, 1995: All India monthly and seasonal rainfall series: 1871–1993. *Theor. Appl. Climatol.,* **49,** 217–224.

Rayner, N. A., E. B. Horton, D. E. Parker, C. K. Folland, and R. B. Hackett, 1996: Version 2.2 of the global sea-ice and sea surface temperature data set, 1903–1994. Climate Research Tech. Note 74, Hadley Centre for Climate Prediction and Research, 21 pp.

Tanaka, M., 1997: Interannual and interdecadal variations of the western North Pacific monsoon and the East Asian Baiu rainfall and their relationship to ENSO cycles. *J. Meteor. Soc. Japan,* **75,** 1109–1123.

Tomita, T., 2000: The longitudinal structure of interannual variability observed in sea surface temperature of the equatorial oceans. *J. Meteor. Soc. Japan,* **78,** 499–507.

——, and T. Yasunari, 1993: On the two types of ENSO. *J. Meteor. Soc. Japan,* **71,** 273–284.

——, and ——, 1996: Role of the northeast winter monsoon on the biennial oscillation of the ENSO/monsoon system. *J. Meteor. Soc. Japan,* **74,** 1–14.

Wallace, J. M., and D. S. Gutzler, 1981: Teleconnections in the geopotential height field during the Northern Hemisphere winter. *Mon. Wea. Rev.,* **109,** 784–812.

——, E. M. Rasmusson, T. P. Mitchell, V. E. Kousky, E. S. Sarachik, and H. von Storch, 1998: On the structure and evolution of ENSO-related climate variability in the tropical Pacific: Lessons from TOGA. *J. Geophys. Res.,* **103,** 14 241–14 259.

Wang, B., and LinHo, 2002: Rainy seasons of the Asian–Pacific monsoon. *J. Climate,* **15,** 386–398.

——, and Q. Zhang, 2002: Pacific–East Asian teleconnection. Part II: How the Philippine Sea anomalous anticyclone is established during El Niño development. *J. Climate,* **15,** 1517–1536.

——, R. Wu, and X. Fu, 2000: Pacific–East Asian teleconnection: How does ENSO affect East Asian climate? *J. Climate,* **13,** 1517–1536.

Xie, P., and P. A. Arkin, 1996: Analyses of global monthly precipitation using gauge observations, satellite estimates, and numerical model predictions. *J. Climate,* **9,** 840–858.

——, and ——, 1997: Global precipitation: A 17-year monthly analysis based on gauge observations, satellite estimates, and numerical model outputs. *Bull. Amer. Meteor. Soc.,* **78,** 2539–2558.

Yoshino, M., 1965: Four stages of the rain season in early summer over East Asia. Part I. *J. Meteor. Soc. Japan,* **43,** 231–245.

——, 1996: Four stages of the rain season in early summer over East Asia. Part II. *J. Meteor. Soc. Japan,* **44,** 209–217.

Zhang, R., A. Sumi, and M. Kimoto, 1996: Impact of El Niño on the East Asian monsoon: A diagnostic study of the '86/87 and '91/92 events. *J. Meteor. Soc. Japan,* **74,** 49–62.